Neuron 52, 595–607, November 22, 2006 ©2006 Elsevier Inc. DOI 10.1016/j.neuron.2006.09.039

Son of Sevenless Directly Links the Robo Receptor to Rac Activation to Control Axon Repulsion at the Midline

Long Yang[1] and Greg J. Bashaw[1,*]
[1] Department of Neuroscience
University of Pennsylvania School of Medicine
421 Curie Boulevard
Philadelphia, Pennsylvania 19104

Summary

Son of sevenless (Sos) is a dual specificity guanine nucleotide exchange factor (GEF) that regulates both Ras and Rho family GTPases and thus is uniquely poised to integrate signals that affect both gene expression and cytoskeletal reorganization. Here, using genetics, biochemistry, and cell biology, we demonstrate that Sos is recruited to the plasma membrane, where it forms a ternary complex with the Roundabout receptor and the SH3-SH2 adaptor protein Dreadlocks (Dock) to regulate Rac-dependent cytoskeletal rearrangement in response to the Slit ligand. Intriguingly, the Ras and Rac-GEF activities of Sos can be uncoupled during Robo-mediated axon repulsion; Sos axon guidance function depends on its Rac-GEF activity, but not its Ras-GEF activity. These results provide in vivo evidence that the Ras and RhoGEF domains of Sos are separable signaling modules and support a model in which Robo recruits Sos to the membrane via Dock to activate Rac during midline repulsion.

Introduction

Correct wiring of the nervous system depends on precisely coordinating the distribution and activity of a diverse set of axon guidance cues and their neuronal receptors. Studies of both invertebrate and vertebrate nervous systems have begun to define the signaling mechanisms that function downstream of guidance receptors to regulate growth cone steering and motility (Patel and Van Vactor, 2002; Yu and Bargmann, 2001). The Rho family of small GTPases (Rac, Rho, and Cdc42) have emerged as central regulators of actin cytoskeletal dynamics in neurons and have been implicated in diverse axon guidance receptor signaling pathways (Dickson, 2001; Luo, 2000; Yuan et al., 2003). Increasing evidence indicates that the positive and negative regulators of the Rho GTPases (GEFs and GAPs) can couple axon guidance receptors to the Rho GTPases to regulate actin dynamics in the growth cone. For example, activation of RhoA downstream of the Eph receptor is mediated by the Rho family GEF—Ephexin1—while Eph-dependent activation of Rac is mediated by another Rho family GEF, Vav (Cowan et al., 2005; Shamah et al., 2001).

Drosophila Robo is the founding member of a conserved group of repulsive guidance receptors of the immunoglobulin (Ig) superfamily and consists of an ectodomain with five Ig domains and three fibronectin type III repeats, a single transmembrane domain, and a long cytoplasmic tail that contains four blocks of conserved cytoplasmic (CC) sequences (CC0, CC1, CC2, CC3) (Bashaw et al., 2000; Kidd et al., 1998). Robo is required to prevent axons from inappropriately crossing the CNS midline in both invertebrates and vertebrates, and it has also been implicated in controlling cell migration in other cell types (Kidd et al., 1998; Kramer et al., 2001; Long et al., 2004). In *Drosophila*, mutations in *robo* and its midline-expressed ligand *slit* result in too many axons crossing and staying at the midline (Kidd et al., 1999; Seeger et al., 1993). Several proteins that regulate the actin cytoskeleton, including the cytoplasmic tyrosine kinase Abelson (Abl) and its substrate Enabled (Ena), contribute to the Robo signaling pathway in *Drosophila* and *C. elegans* (Bashaw et al., 2000; Hsouna et al., 2003; Wills et al., 2002; Yu et al., 2002). In addition, genetic interaction and biochemical experiments in *Drosophila* and biochemical experiments in mammalian cell culture indicate that activation of Slit-Robo signaling leads to activation of Rac and Rho, and inactivation of Cdc42 (Fan et al., 2003; Fritz and VanBerkum, 2002; Matsuura et al., 2004; Wong et al., 2001).

It is clear from studies of Slit-mediated neural precursor cell migration in rats that inactivation of Cdc42 by Robo is mediated by *S*lit-*R*obo GAP (SrGAP1) (Wong et al., 2001). However, how Slit leads to the activation of Rac in either *Drosophila* or vertebrate systems is still unknown. Recent work in *Drosophila* suggests that the SH3-SH2 adaptor protein Dock may play a role in recruiting Rac to the Robo receptor. Slit stimulation recruits Dock and p21-activated kinase (Pak) to the Robo receptor, and Pak is a downstream target of Rac. It has been proposed that Dock recruits Pak to specific sites at the growth cone membrane, where Pak, activated by Rac, regulates the recycling and retrograde flow of actin filaments (Fan et al., 2003; Hing et al., 1999). Despite these observations, it still remains unclear how Rac is activated in this context. One possible mechanism would be by negative regulation of a Rac-specific GAP(s) upon Slit stimulation. Indeed, a genome-wide analysis in *Drosophila* has identified a Rac-specific GAP, CrossGAP/Vilse (CrGAP), which interacts directly with the CC2 motif of Robo (Hu et al., 2005; Lundstrom et al., 2004). Overexpression of *crGAP* mimics the *robo* mutant phenotype, which suggests that it plays a negative role in Slit-Robo signaling. However, *crGAP/vilse* mutants do not have major midline axon guidance defects; in fact, loss of *crGAP/vilse* actually leads to mild *robo*-like defects (Lundstrom et al., 2004). Thus, it would appear that downregulating *crGAP* alone in the Robo signaling pathway is not sufficient to lead to activation of Rac.

Since Rho GTPases are directly activated by GEFs, we wondered whether Slit-dependent upregulation of a Rac-specific GEF leads to the activation of Rac. Among the 22 Rho family GEFs in the *Drosophila* genome, Sos is a good candidate to play this role for the following reasons. First, *sos* is among eight RhoGEFs that are enriched in the *Drosophila* embryonic central

*Correspondence: gbashaw@mail.med.upenn.edu

nervous system (Hu et al., 2005). Second, *sos* was previously shown to genetically interact with *slit* during midline guidance (Fritz and VanBerkum, 2000); no other GEF has been shown to genetically interact with *slit* or *robo*. Third, mutations in *sos* partially suppress the *commissureless* mutant phenotype, where elevated *robo* function results in a complete absence of axon commissures, suggesting that *sos* functions in the *robo* pathway (Fritz and VanBerkum, 2000). Finally, mammalian Sos is a Rac-specific GEF and it directly binds to Nck, the mammalian homolog of *Drosophila* Dock (Hu et al., 1995; Nimnual et al., 1998; Okada and Pessin, 1996).

Sos was identified in *Drosophila* as a GEF for Ras in the sevenless signaling pathway during the development of the *Drosophila* compound eye, where it activates the Ras signaling cascade to determine R7 photoreceptor specification (Bonfini et al., 1992; Simon et al., 1991). Studies in mammalian cell culture demonstrated that Sos functions as a GEF for both Ras and Rac in the growth factor-induced receptor tyrosine kinase (RTK) signaling cascade (Nimnual and Bar-Sagi, 2002; Nimnual et al., 1998). Upon RTK activation, the SH3/SH2 adaptor protein Grb2/Drk recruits Sos to autophosphorylated receptors at the plasma membrane, where Sos activates membrane-bound Ras. In a later event downstream of RTK activation, Sos is thought to be targeted to submembrane actin filaments by interaction with another SH3 adaptor, E3b1(Abi-1), where Sos activates Rac (Innocenti et al., 2002, 2003; Scita et al., 1999, 2001). Whether the activation of Rac by Sos is strictly dependent on prior activation of Ras remains controversial, nor is it clear how Sos coordinates the activity of its two GEF domains in vivo.

Here we present evidence that Sos functions as a Rac-specific GEF during *Drosophila* midline guidance. Sos is enriched in developing axons, and *sos* exhibits dosage-sensitive genetic interactions with *slit* and *robo*. Strikingly, genetic rescue experiments show that the Dbl homology (DH) RhoGEF domain of Sos, but not its RasGEF domain, is required for its midline guidance function. Biochemical experiments show that Sos physically associates with the Robo receptor through Dock in both mammalian cells and *Drosophila* embryos. Furthermore, Slit stimulation of cultured cells results in the rapid recruitment of Sos to membrane Robo receptors. These results provide a molecular link between the Robo receptor and Rac activation, reveal an independent in vivo axon guidance function of the DH RhoGEF domain of Sos, and support the model that Slit stimulation recruits Sos to the membrane Robo receptor via Dock to activate Rac-dependent cytoskeletal changes within the growth cone during axon repulsion.

Results

Sos Is Enriched in CNS Axons and Interacts Genetically with *slit* and *robo*

It has been reported that Sos protein is enriched in the axons of stage 16 *Drosophila* embryos (Fritz and VanBerkum, 2000), a stage when most axons have already made their midline guidance decisions. Therefore, we examined Sos expression at earlier stages. In stage 12 wild-type embryos, when axons start to project, Sos is broadly expressed in most cells but begins to be enriched in developing axons as revealed by double-staining with BP102 (Figures 1A–1C). By stage 17, there is a strong enrichment of Sos in all CNS axons, including longitudinal axons and commissural axons (Figures 1D–1F). In *sos* zygotic null mutants, the overall Sos protein level is significantly reduced, but there is still a considerable amount of Sos remaining in CNS axons (Figures 1G and 1H). Interestingly, Sos is also enriched in tracheal cells (Figures 1D and 1F), whose migration is regulated by Slit-Robo signaling as well (Englund et al., 2002).

To investigate the potential role of Sos in Slit-Robo-mediated *Drosophila* midline axon guidance, we analyzed the phenotype of *sos* mutants and tested for genetic interactions between *sos*, *slit*, and *robo*. In wild-type embryos, Fasciclin II (FasII)-positive axons project longitudinally and never cross the midline (Figures 2A and 2F). In *robo* mutants, FasII-positive axons inappropriately cross the midline many times (Figure 2B). Consistent with previous results (Fritz and VanBerkum, 2000), two independent *sos* null mutants have mild midline crossing defects that are strongly enhanced by reducing the gene dose of *slit* or *robo* (Figures 2C–2F). Importantly, these interactions are dosage sensitive: removing one copy of *sos* and one copy of *slit* or *robo* did not cause any axon guidance defects, while removing both copies of *sos* and one copy of *slit* or *robo* did. Here it is important to recall that, even though we are removing both zygotic copies of *sos*, there is still a considerable amount of Sos protein remaining in these embryos (Figure 1G). The midline crossing defects observed in *sos* mutants together with these dosage-sensitive genetic interactions suggest that *sos* may contribute to Slit-Robo repulsion.

Since *Drosophila sos* is involved in cell fate specification, the guidance defects in *sos* mutants might be due to malfunctions in other processes rather than axon guidance itself. To rule out this possibility, a genetic rescue approach using the Gal4/UAS system was taken (Brand and Perrimon, 1993). Since *sos* mutants have only weak axon guidance defects, we performed rescue experiments in the stronger sos^{e2H}, $slit^{2}/sos^{e4G}$ mutant background by expressing *UASSosmyc* under the control of a neuronal-specific *fushi-tarazu neurogenic Gal4* ($ftz^{ng}Gal4$) driver. The $ftz^{ng}Gal4$ driver expresses *Gal4* in subsets of ipsilaterally projecting neurons. We found that the ectopic midline crossing phenotype of sos^{e2H}, $slit^{2}/sos^{e4G}$ was significantly rescued in embryos that carried the wild-type *sos* transgene (Figure 2F). Using several different transgene inserts, we found that the extent of rescue correlated with the level of transgene expression (data not shown). Taken together, these results strongly suggest that the neuronal-specific function of Sos is important for Slit-Robo-mediated midline axon repulsion.

It seems likely that the strong maternal deposit of *sos* in developing embryos could account for the relatively weak midline axon guidance defects observed in *sos* zygotic mutants. Due to the requirement of Sos during early development, embryos lacking both maternal and zygotic *sos* have severe patterning defects (Luschnig et al., 2004; Silver et al., 2004), making it difficult to determine the full contribution of Sos to axon guidance. RNAi experiments to more completely block *sos*

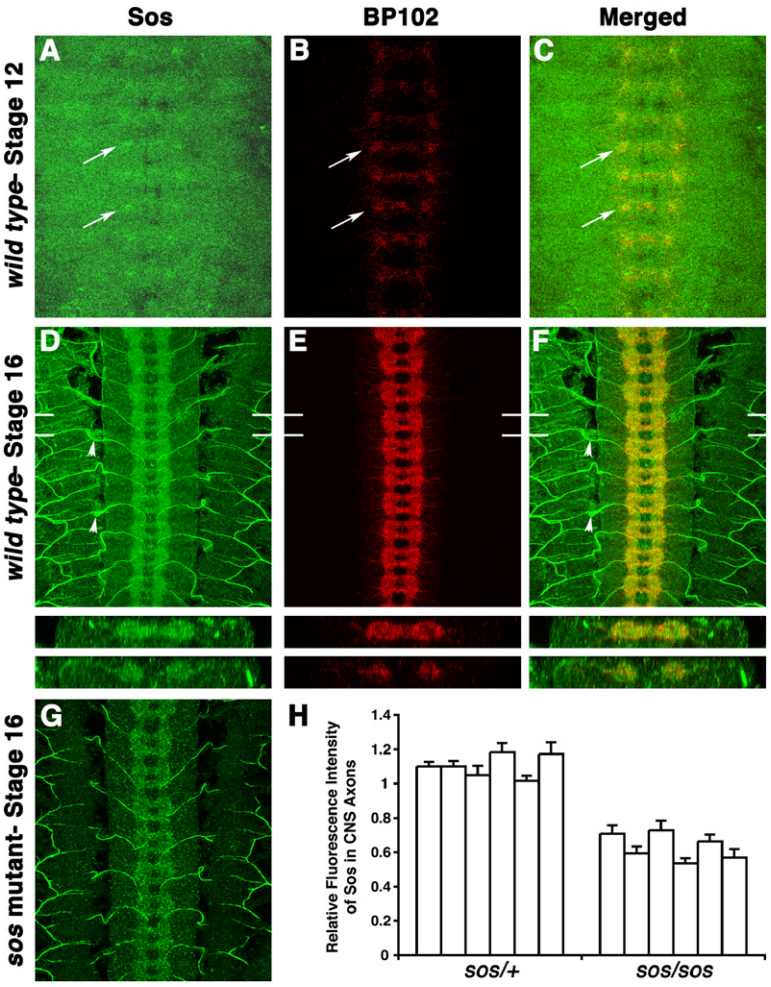

Figure 1. Sos Protein Expression in Wild-Type and *sos* Mutants

Wild-type stage 12 (A–C) or stage 16 (D–F) embryos costained with rabbit anti-Sos and MAb-BP102. Anterior is up. (A) Sos staining. Sos is broadly expressed in most cells and starts to be enriched in developing axons (white arrows). (B) BP102 staining of the same embryo shows developing CNS axons (white arrows). (C) An overlay of the two staining patterns reveals localization of Sos in developing CNS axons (white arrows). (D–F) A wild-type stage 16 embryo costained with anti-Sos and MAb-BP102. Sos protein is strongly enriched in CNS axons and trachea (arrowheads). Note the clear localization of Sos proteins in both commissural axons and longitudinal axons shown by the two XZ sections, which are magnified by 2×. (G) A sos^{e2H} mutant stage 16 embryo stained with rabbit anti-Sos. Note that Sos protein levels are much reduced in both CNS axons and trachea. (H) Quantification of relative fluorescence intensity of Sos proteins revealed that the relative fluorescence intensity of Sos was reduced from 1.1 in heterozygous mutant embryos to 0.6 in homozygous mutant embryos. Six random pairs of sos^{e2H} mutant embryos and their heterozygous siblings (sos^{e2H}/+) are shown on the x axis. Relative florescence intensity of Sos in CNS axons of each embryo is calculated as absolute Sos fluorescence intensity divided by absolute BP102 fluorescence intensity. Absolute fluorescence intensity is measured from a single confocal XZ section. The average value of six independent hemisegments, including three commissural segments and three non-commissural segments of each embryo, is shown on the y axis. Error bars represent standard error of the mean.

function did lead to much stronger midline crossing defects; however, these manipulations also resulted in additional patterning defects that complicate the interpretation of these results (L.Y. and G.J.B., unpublished data).

Drosophila Sos Functions as a Rac-Specific GEF In Vivo

Drosophila Sos is highly homologous to mammalian Sos and contains all the conserved functional domains. To test if *Drosophila* Sos, like its mammalian homolog, can activate small Rho family GTPases in vivo and to determine its substrate preference, we took advantage of the fact that when *rac1*, *rhoA*, or *cdc42* is overexpressed in the developing eye, a "rough eye" phenotype is induced because of a disruption of ommatidial cell development (Figures S1C, S1E, and S1G in the Supplemental Data available with this article online) (Hariharan et al., 1995; Nolan et al., 1998). The "rough eye" phenotype caused by overexpression of *rac1* was strongly enhanced by coexpression of *sos* (Figures S1C and S1D). This enhancement is specific for *rac1*, as coexpressing *sos* with *rhoA* or *cdc42* did not modify the rough eye phenotype (Figures S1E–S1H). This result indicates that *Drosophila* Sos can specifically activate Rac in the developing eye, which is consistent with the in vitro data that mammalian Sos only displays GEF activity toward Rac, but not RhoA and Cdc42 (Nimnual et al., 1998).

Next, we asked which small GTPase is likely to be the in vivo target of Sos during midline axon guidance, since all three members of the Rho family of small Rho GTPases (Rac, Rho, Cdc42) have been implicated in Slit-Robo repulsion. Both genetic and biochemical evidence indicates that activation of Slit-Robo signaling leads to activation of Rac and Rho, and inactivation of Cdc42 (Fan et al., 2003; Wong et al., 2001). Since the *sos* mutant phenotype and its genetic interaction with *slit* and *robo* (Figure 2; Table S1) suggest that Sos may play a positive role in Slit-Robo signaling, we focused on determining whether Rac or RhoA is the in vivo target for Sos during midline axon guidance. Panneuronal overexpression (using *elavGal4*) of *RacDN* (*UASRac*^{N17}), or *RhoADN* (*UASRhoA*^{N19}), in an otherwise wild-type background did not result in significant ectopic midline crossing. However, both the *RacDN* and the *RhoADN* showed strong enhancement of midline guidance defects seen in *sos* homozygous mutants (Table S1). This result is consistent with the previous finding that overexpressing either *RacDN* or *RhoADN* with the *ftz*^{ng}*Gal4* driver enhances the *sos* mutant phenotype to the same extent (Fritz and VanBerkum, 2002), suggesting

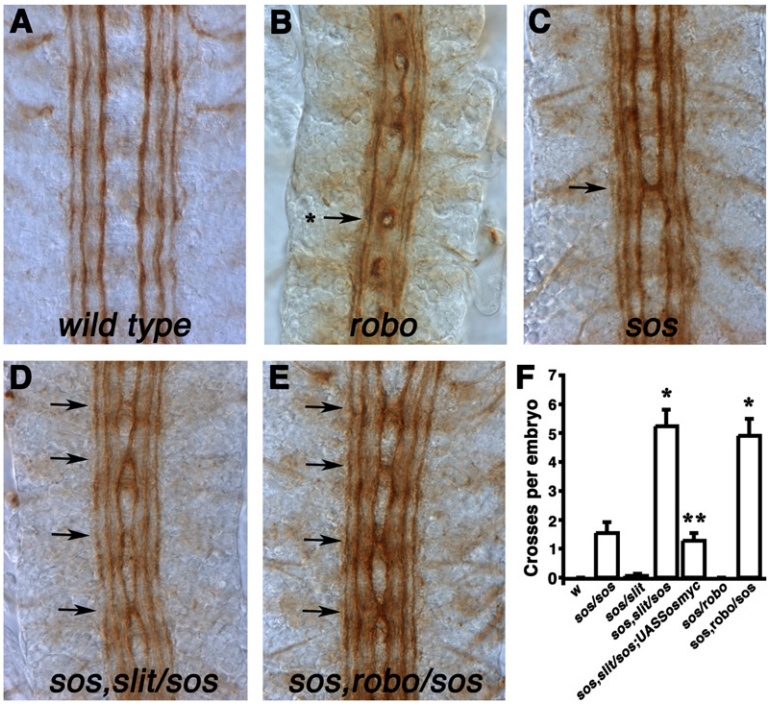

Figure 2. Genetic Interactions between *slit*, *robo*, and *sos*

(A–E) Stage 16 embryos stained with anti-FasII to reveal a subset of longitudinal axons. Anterior is up. Partial genotypes are indicated at the bottom of each panel. (A) A wild-type embryo. No FasII-positive axon bundles cross the midline. (B) A $robo^{GA285}$ mutant embryo. The innermost FasII bundle wanders back and forth across the midline (arrows with asterisks). (C) A sos^{e2H}/sos^{e4G} mutant embryo with a weak midline crossing defect. An arrow indicates a single bundle of axons that abnormally crosses the midline. (D) sos^{e2H}, $slit^{2}/sos^{e4G}$ embryos show a strong enhancement of midline guidance defects with more bundles of axons inappropriately crossing the midline (arrows). Compare with (C). (E) sos^{e2H}, $robo^{GA285}/sos^{e4G}$ embryos show similar enhancement of midline guidance defects.

(F) A quantitative analysis of FasII guidance defects. Partial genotypes are indicated on the x axis. Average number of ectopic crosses per embryo is shown on the y axis. Asterisks denote that phenotypes that are statistically different from *sos* mutants ($p < 0.0001$ in a two-sample Student's t test). Note that FasII guidance defects in sos^{e2H}, $slit^{2}/sos^{e4G}$ can be rescued by expressing *UASSosmyc* under the control of a neuronal-specific $ftz^{ng}Gal4$ driver. Double asterisks denote that this neuronal rescue is of statistical significance ($p < 0.0001$, two-sample Student's t test). Error bars represent standard error of the mean.

that Sos could activate both Rac and Rho during midline guidance.

A major concern of using this type of dominant-negative approach is its nonspecificity. Dominant-negative forms of the Rho GTPases are thought to act by sequestering endogenous GEFs. Since different Rho GTPases may share common GEFs, it is not clear whether the observed genetic interactions could reflect simultaneous downregulation of multiple Rho GTPases. To resolve this issue, we examined the effects of "loss-of-function" mutations of *rac1* or *rhoA* in *sos* homozygous mutant embryos. Loss-of-function mutants of *rac1* ($rac1^{J11/J11}$) or *rhoA* ($rhoA^{220/220}$) alone did not result in obvious midline guidance defects (Figures 3B and 3D; Table S1). However, removing only one copy of *rac1* strongly enhanced the ectopic midline crossing phenotype seen in *sos* mutants (Figures 3A and 3C). Considering that there are three redundant *rac* genes (*rac1*, *rac2*, and *mtl*) in *Drosophila* (Hakeda-Suzuki et al., 2002; Ng et al., 2002), it is particularly striking that $sos^{e2H/e2H}$; $rac1^{J11}$/+ mutants exhibit such strong defects (Figure 3G). Indeed, the greater than 5-fold increase in ectopic midline crossing is likely to underestimate the total defects, as some segments are fused in these mutants, and fused segments were only counted as one ectopic cross in our quantification scheme (Figure 3C). In contrast, removing one copy of *rhoA* did not show any effect on the *sos* mutant phenotype, and removing two copies of *rhoA* resulted in only a modest enhancement of the ectopic crossing defects, which were much weaker than $sos^{e2H/e2H}$; $rac1^{J11}$/+ mutants (Figures 3A, 3D, 3F, and 3G). Based on this highly sensitive loss-of-function genetic interaction between *sos* and *rac1*, but not *rhoA*, we conclude that Rac is the preferred substrate for Sos during midline guidance; however, these observations do not formally exclude the possibility that Sos also activates Rho to a lesser extent during midline guidance.

Sos Functions in Opposition to CrGAP/Vilse

Since CrGAP/Vilse is a Rac-specific GAP in the Robo signaling pathway (Hu et al., 2005; Lundstrom et al., 2004), we would predict that Sos plays an opposing role to CrGAP/Vilse. Consistent with published results (Hu et al., 2005), low-level overexpression of *crGAP/vilse* (one copy of *UASCrGAP* and one copy of *elavGal4* driver) results in a wild-type FasII axon projection pattern (Figure 4A). High-level overexpression of *crGAP/vilse* (two copies of *UASCrGAP* and two copies of *elavGal4* driver) results in a series of defects, including extensive ectopic midline crossing in some segments, which is reminiscent of the *robo* mutant phenotype, and axon outgrowth defects in some segments, which is similar to triple loss-of-function *rac* mutants (Hakeda-Suzuki et al., 2002; Ng et al., 2002) (Figure 4C). If Sos does play an opposing role to CrGAP/Vilse in regulating Rac activity, we would expect that reducing the levels of *sos* should enhance the axon guidance defects in embryos with low-level overexpression of *crGAP/vilse*, while overexpressing *sos* should suppress the axon guidance and outgrowth defects caused by high-level overexpression of *crGAP/vilse*. This is indeed the case. Removing two copies of *sos* in embryos expressing low levels of *crGAP/vilse* led to a striking enhancement of ectopic midline crossing and axon outgrowth

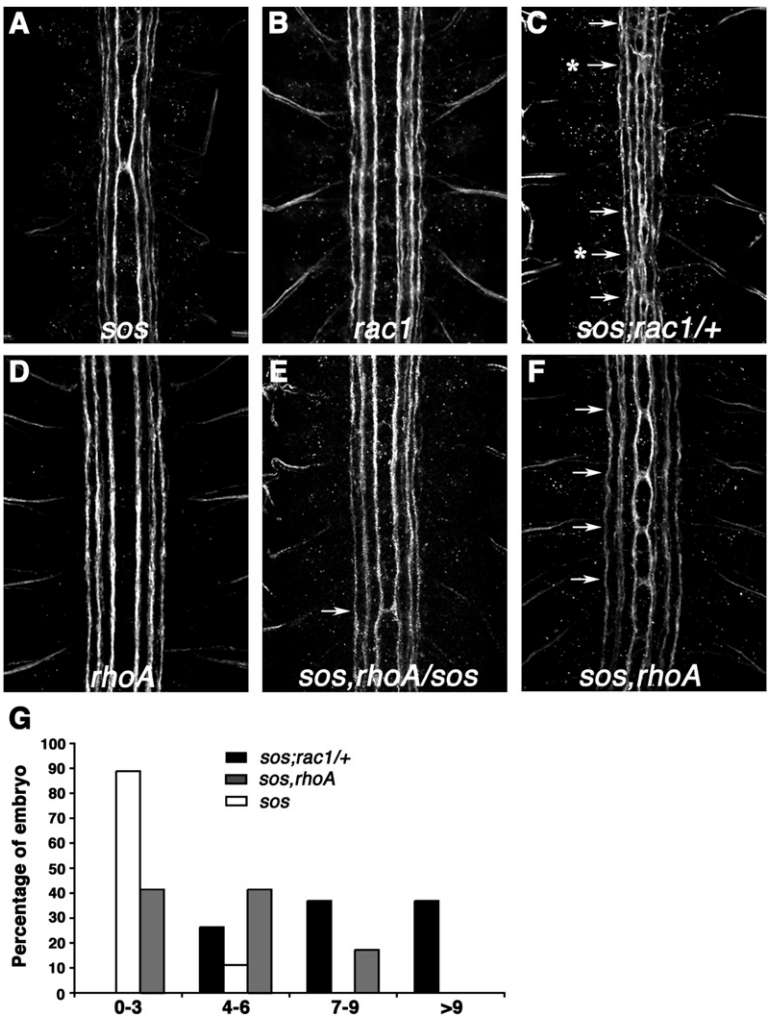

Figure 3. Genetic Interactions between *sos*, *rac1*, and *rhoA*

(A–F) Stage 16 embryos stained with anti-FasII to reveal a subset of longitudinal axons. Anterior is up. Partial genotypes are indicated at the bottom of each panel. (A) sos^{e2H} mutant embryos showing a mild midline guidance defect. An arrow indicates a single bundle of axons that crosses the midline. (B) A $rac1^{J11}$ mutant embryo. The FasII-positive axons appear to be wild-type. (C) sos^{e2H}; $rac1^{J11}$/+ mutant embryos show strong enhancement of midline guidance defects with more bundles of axons inappropriately crossing the midline (arrows) or fused together (arrows with asterisks). Compare to (A). Analysis of these embryos with antibodies to several glial and neuronal markers did not reveal any overall patterning defects (data not shown). (D) A $rhoA^{220}$ mutant embryo. The FasII axons appear to be wild-type. (E) sos^{e2H}, $rhoA^{220}$/sos^{e2H} embryos show a similar extent of midline guidance defects as in sos^{e2H} mutant embryos. An arrow indicates a single bundle of axons that crosses the midline. (F) sos^{e2H}, $rhoA^{220}$ double mutant embryos show stronger midline guidance defects with more axon bundles inappropriately crossing the midline (arrows) compared to sos^{e2H} mutant embryos (A), but much less severe defects than sos^{e2H}; $rac1^{J11}$/+ mutant embryos (C).

(G) A graphic representation of the quantitative analysis of FasII guidance defects. The x axis represents the severity of the crossing phenotype, and the y axis represents the percentage of embryos observed for the indicated phenotypic class.

defects (Figures 4A, 4B, and 4E; Table S1). On the other hand, panneuronal overexpression of *UASSosmyc* in embryos expressing high levels of *crGAP/vilse* rescued both of these defects (Figures 4C–4E; Table S1). Together, these observations suggest that activation of Rac downstream of Robo is tightly regulated by both GEF and GAP activities.

The Guidance Function of Sos Is Dependent on Rac, but Not Ras Activation

Although the results we have presented support the idea that Sos functions as a Rac-GEF during Robo repulsive axon guidance, it remains unclear whether the *sos* axon guidance function is also dependent on Ras activation. Although previous genetic studies failed to detect dose-dependent genetic interactions between *ras* and *robo* (Fritz and VanBerkum, 2000), there are several reasons to give serious consideration to this possibility. First, studies of other repulsive axon guidance receptor signaling pathways have revealed an important role for Ras activation. For example, Plexin-B1 mediates Sema4D-induced repulsive axon guidance signaling in part through the activation of Ras (Oinuma et al., 2004a, 2004b). Second, it is not clear whether the Rac-GEF activity of Sos is gated by Sos-dependent Ras activation. For example, in the canonical RTK→Sos→Ras→Sos→Rac pathway, Sos couples Ras activation to the subsequent activation of Rac (Innocenti et al., 2002, 2003; Nimnual et al., 1998). Alternatively, other studies suggest that Rac activation after growth factor treatment could occur in a Ras-independent manner, RTK→Sos→Rac, in which the Ras-GEF activity of Sos seems not to be required for its Rac-GEF activity (Scita et al., 2000; Sini et al., 2004). Our genetic model system provides an excellent opportunity to test in vivo whether the Ras and Rac-GEF activities of Sos can be functionally uncoupled.

To test whether or not the Ras-GEF activity of Sos is required for the activation of Rac, we took advantage of the observation that the axon guidance defects caused by removing one copy of *slit* in a *sos* mutant background can be rescued by overexpressing wild-type Sos (Figures 5A, 5B, and 5J). Two mutant versions of *Sos*, *UASSosΔDHmyc* and *UASSosΔRasGEFmyc*, were generated and examined for their ability to rescue sos^{e2H}, $slit^{2}$/sos^{e4G} mutants (Figure 5I). The expression level of transgenes was determined by western blot (Figure S2D), and transgene localization was determined by anti-myc staining (Figures S2A–S2C). Mutant transgenes with comparable expression levels and

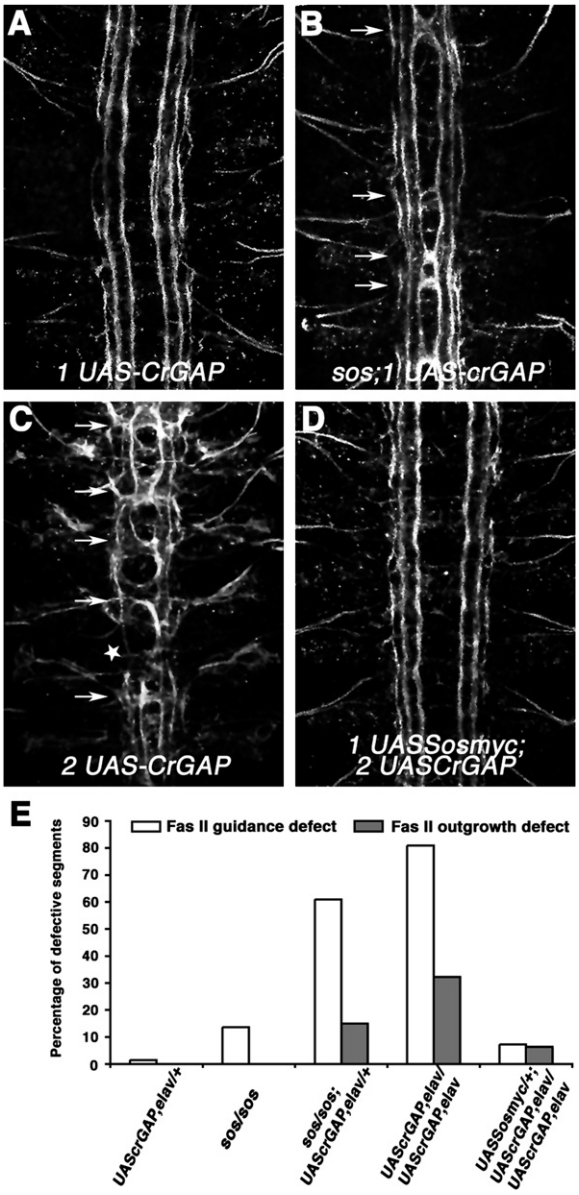

Figure 4. Genetic Interaction between *sos* and *crGAP/vilse*

(A–D) Stage 16 embryos stained with anti-FasII to reveal a subset of longitudinal axons. Anterior is up. Partial genotypes are indicated at the bottom of each panel. (A) A wild-type embryo expressing one copy of *UASCrGAP* and one copy of *elavGal4*. The FasII axon projections appear to be normal. (B) A sos^{e2H} mutant embryo expressing one copy of *UASCrGAP* and one copy of *elavGal4.* An enhancement of ectopic midline crossing is observed (arrows). (C) wild-type embryos expressing two copies of *UASCrGAP* and two copies of *elavGal4* show severe FasII axon guidance defects (arrows) and FasII axon outgrowth defect (stars). (D) Embryos expressing *UASSosmyc* together with two copies of *UASCrGAP* and two copies of *elavGal4* rescue both the guidance and outgrowth defects.

(E) A graphic representation of the quantitative analysis of the guidance and outgrowth defects. Genotypes are indicated on the x axis. Percentage of defective segments (n > 16; see Table S1) is represented on the y axis.

localization were used in the rescue experiments. Overexpression of *UASSosΔDHmyc* could not rescue the axon defects in sos^{e2H}, $slit^{2}/sos^{e4G}$ mutants (Figures 5A, 5C, and 5J). In contrast, overexpression of *UASSosΔRasGEFmyc* significantly rescued sos^{e2H}, $slit^{2}/sos^{e4G}$ mutants (Figures 5A, 5D, and 5J). To exclude the possibility that the differential rescue effects of truncated Sos transgenes are dependent on particular genetic backgrounds or Gal4 drivers, we performed the same genetic rescue experiment in the *sos, rhoA* double mutant background using a panneuronal driver (*elavGal4*). Similar rescue effects were observed (Figure 5E, 5F, and 5J). Taken together, these results reveal that the Rac-GEF activity of Sos, but not its Ras-GEF activity, is required for its function in Robo repulsive signaling and provide strong in vivo evidence that the Ras and Rac-GEF activities of Sos can be functionally uncoupled during signal transduction.

Dock Physically Couples Sos to the Robo Receptor

While the genetic results we have presented suggest that Sos functions to activate Rac in the Robo signaling pathway, it remains unclear how and whether Sos is linked to the Robo receptor. We first examined the possibility that Sos directly binds to Robo, but we failed to detect any physical interaction by coimmunoprecipitation from 293T cells coexpressing Robo and Sos (Figure 6C). We next considered the possibility that other components of the Robo signaling pathway could serve as links between Robo and Sos. Since *ena* and *dock* are both implicated in Robo signaling (Bashaw et al., 2000; Fan et al., 2003; Yu et al., 2002), and they appear to function independently of each other, we tested whether either of these genes displayed dose-dependent genetic interactions with *sos.* Reducing the dose of *dock* enhanced the *sos* mutant phenotype, while similar reduction of *ena* had no effect (Table S1). These genetic data suggest that Sos might function as a Rac-GEF in Dock-dependent repulsive signal transduction downstream of Robo. Other lines of evidence also support this idea. First, Dock has been implicated in the increase in Rac activity caused by Slit stimulation, since the ΔCC2ΔCC3 mutant version of Robo that cannot bind to Dock is unable to mediate the Slit-dependent increase in Rac activity (Fan et al., 2003). Second, mammalian Sos has been shown to directly bind to Nck, the homolog of Dock (Hu et al., 1995; Okada and Pessin, 1996).

Therefore, we examined the physical association between Sos and Dock in 293T cells. Both GST pull-down and coimmunoprecipitation assays revealed that Sos physically associates with Dock (Figures 6A and 6B). In a yeast two-hybrid assay, the direct binding of Dock to Sos was also detected, and the binding domain for each protein was determined. We found that the C-terminal portion of Sos that contains the PXXP motif directly interacts with the SH3-2 and SH3-3 domains of Dock (Figure 6D and 6E). Since the SH3-1 and SH3-2 domains of Dock are required for binding to Robo (Fan et al., 2003), we would predict that a Robo-Dock-Sos ternary complex can form, in which Dock bridges the interaction between Robo and Sos. This is indeed the case. In 293T cells, when Dock is coexpressed with Robo and Sos, formation of a Robo-Dock-Sos protein complex is detected by coimmunoprecipitation (Figure 6F). Furthermore, in *Drosophila* embryo lysates, endogenous Sos and Dock are detected in a complex with Robo (Figure 6G), suggesting that this protein

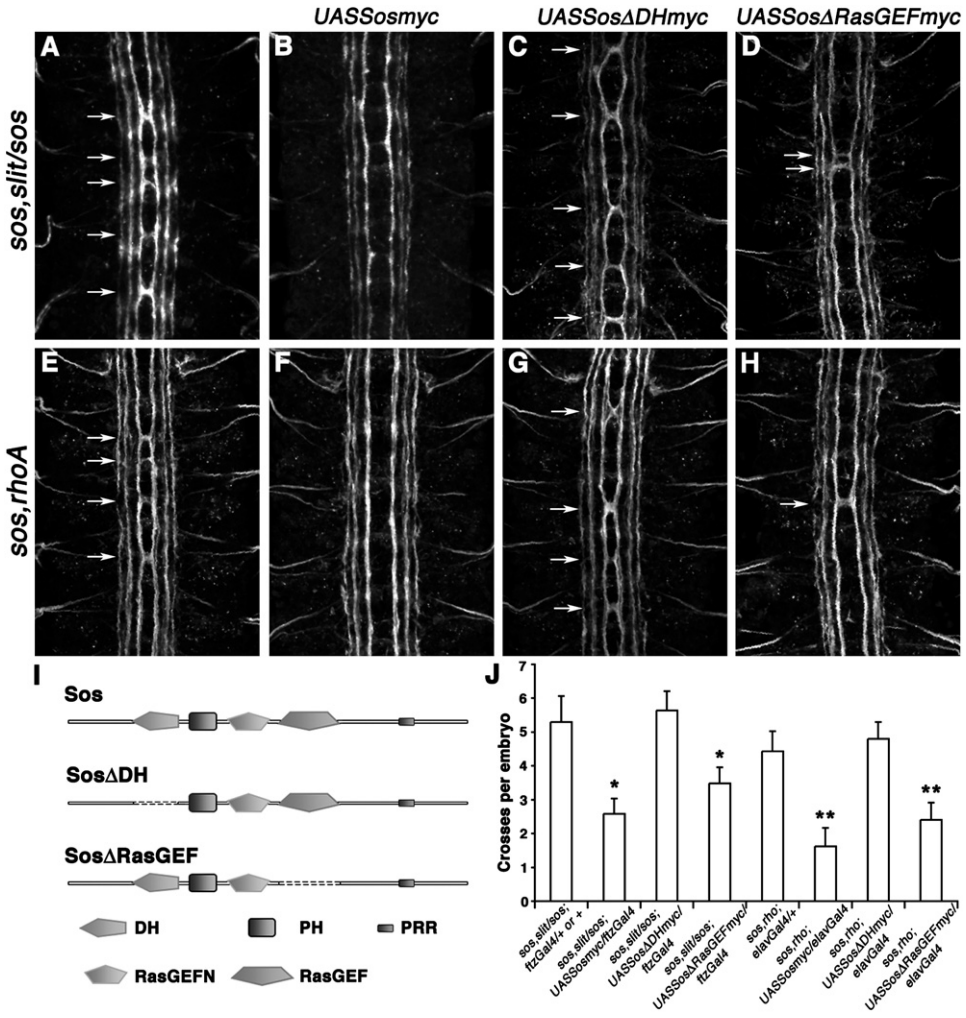

Figure 5. The Midline Guidance Function of Sos Is Dependent on Its DH RhoGEF Domain

(A–H) Stage 16 embryos stained with anti-FasII to reveal a subset of longitudinal axons. Anterior is up. Partial genotypes for rescue are indicated to the left of the micrographs, and different rescue transgenes are indicated on the top. (A) A sos^{e2H}, $slit^{2}/sos^{e4G}$; $ftz^{ng}Gal4$ *or TM2*/+ embryo with ectopic midline crosses indicated by arrows. (B) A sos^{e2H}, $slit^{2}/sos^{e4G}$, *UASSosmyc*/$ftz^{ng}Gal4$ embryo or sos^{e2H}, $slit^{2}/sos^{e4G}$; *UASSosΔRasGEFmyc*/$ftz^{ng}Gal4$ (D) shows the neuronal rescue of the midline guidance defect by *UASSosmyc* or *UASSosΔRasGEFmyc*. (C) A sos^{e2H}, $slit^{2}/sos^{e4G}$; *UASSosΔDHmyc*/$ftz^{ng}Gal4$ embryos with ectopic midline crosses (arrows) indicate that *UASSosΔDHmyc* failed to rescue the guidance defect observed in sos^{e2H}, $slit^{2}/sos^{e4G}$ mutant embryos. (E–H) Similar rescue effects of the different transgenes were observed in rescuing the ectopic midline crossing in sos^{e2H}, $rhoA^{220}$ double mutants under the control of the *elavGal4* driver.

(I) A schematic representation of Sos wild-type and mutant transgenes used in these genetic rescue experiments. DH, Dbl homology domain; PH, pleckstrin homology domain; PRR, proline-rich region. A 6-myc tag was added to the C terminus of each transgene (not shown) to monitor expression levels in embryos.

(J) A quantitative analysis of FasII guidance defects. Genotypes are indicated on the x axis. The average number of ectopic crosses per embryo is shown on the y axis. Asterisks denote the phenotypes that are statistically different from sos^{e2H}, $slit^{2}/sos^{e4G}$, $ftz^{ng}Gal4$, or *TM2*/+ embryo mutants ($p < 0.05$ in a two-sample Student's t test). Double asterisks denote that phenotypes that are statistically different from sos^{e2H}, $rhoA^{220}$; *elavGal4*/+ mutants ($p < 0.01$ in a two-sample test). The rescue effects of *UASSosmyc* and *UASSosΔRasGEFmyc* are not statistically different for either the sos^{e2H}, $slit^{2}/sos^{e4G}$ background ($p = 0.09$) or the sos^{e2H}, $rhoA^{220}$ background ($p = 0.18$). Error bars represent standard error of the mean.

complex exists under physiological conditions, and that it is not just an artifact when proteins are overexpressed in mammalian cells.

Slit Stimulation Triggers the Recruitment of Sos to Membrane Robo Receptors and Induces Membrane Ruffles and Lamellipodia Formation

The genetic and biochemical data that we have presented, together with previously published data indicating that Slit stimulation leads to enhanced Dock recruitment and increased Rac activity (Fan et al., 2003), support the model that Sos is recruited to the Robo receptor where it activates Rac (and possibly Rho) to promote midline repulsion. If this model were true, we would predict that Slit activation of Robo at the plasma membrane should lead to the recruitment of Sos to membrane Robo receptors and induce changes in actin morphology. To test this prediction, we turned to a mammalian HEK293T cell culture system where both the subcellular distribution of Sos and actin morphology have been well characterized. Studies from mammalian cell culture reveal that the Rac-GEF activity of Sos is tightly

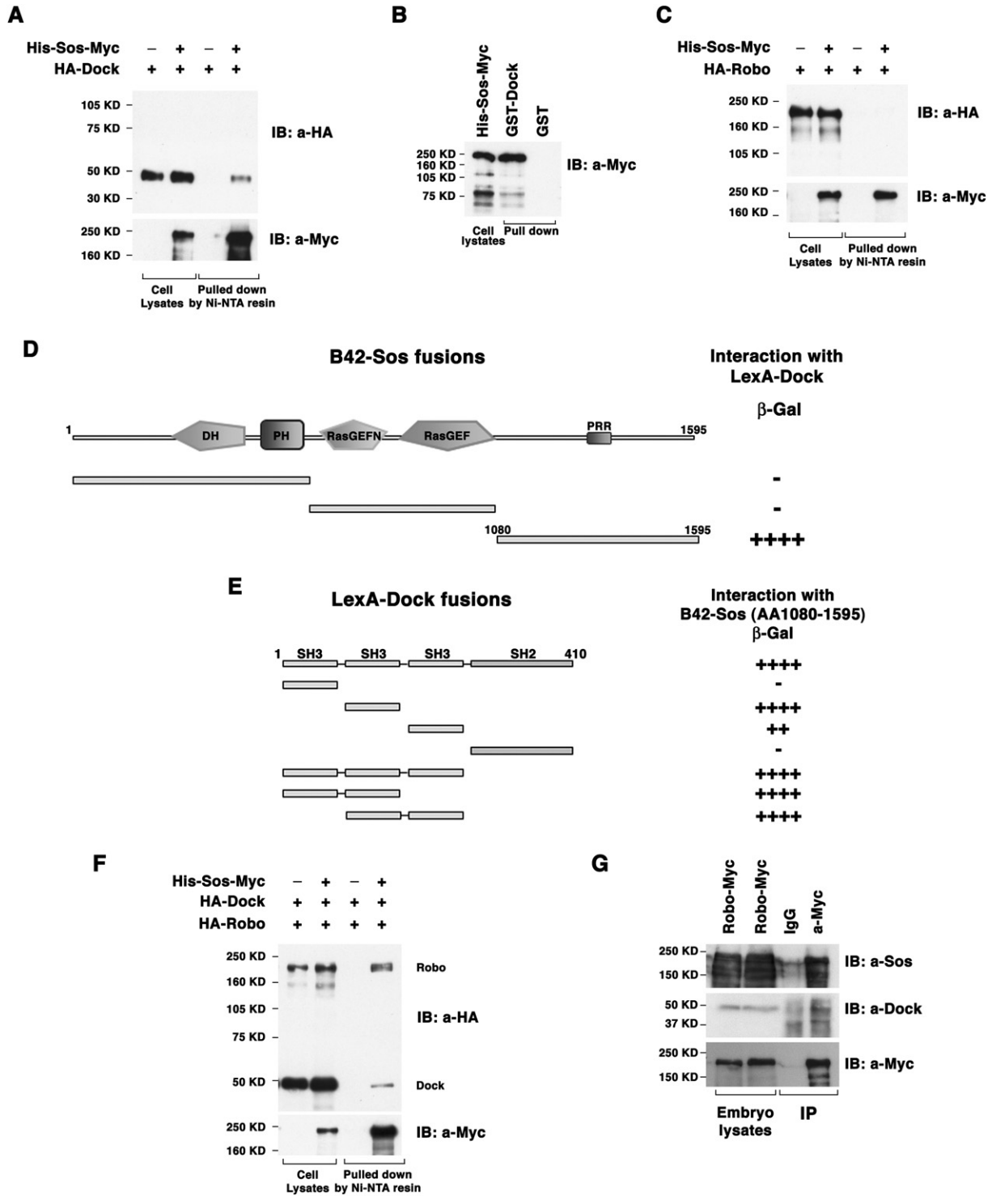

Figure 6. Dock Physically Couples Sos to the Robo Receptor

(A and B) Interactions between Sos and Dock in 293T cells. (A) 293T cell lysates coexpressing His-Sos-Myc and HA-Dock, or HA-Dock alone, were precipitated by Ni-NTA beads. The right two lanes show the coprecipitated proteins, while the left two lanes indicate Sos and Dock expression in cells. (B) 293T cell lysates expressing His-Sos-Myc were precipitated by Glutathione Sepharose 4B beads bound to GST or GST-Dock. The right two lanes show the coprecipitated proteins, while the leftmost lane indicates Sos expression in cells. (C) 293T cell lysates coexpressing His-Sos-Myc and HA-Robo, or HA-Robo alone, were precipitated by Ni-NTA beads. The right two lanes show that Robo is not coprecipitated with Sos, while the left two lanes indicate Sos and Robo expression in cells. (D) Different sized forms of Sos were fused to the B42 transcription activation domain. Full-length Dock was fused to the LexA DNA binding domain. Our analysis indicates that the C-terminal part of Sos, which includes the conserved proline-rich regions, is important for the Sos-Dock physical interaction. PRR, proline-rich region. (E) The same strategy was used to identify the potential interacting domain in Dock for Sos. LexA-fused truncated forms of Dock were tested with B42-Sos. Strong binding was mediated by the SH3-2 or SH3-3 domains. Yeast turned dark blue (++++; strong interaction), blue (+++), light blue (++), or white

regulated, and that it is dependent on the precise subcellular localization of Sos. In resting cells, Sos is predominantly localized to the cytoplasm, and its Rac-GEF activity is inhibited. In growth factor-treated cells, Sos is recruited to the membrane, where its Rac-GEF activity induces a specific actin morphology—membrane ruffles and lamellipodia, a hallmark of Rac activation. In human Robo1-expressing 293T cells after control treatment, endogenous Sos shows a similar predominantly cytoplasmic localization (Figures 7E–7H) as in non-hRobo1-expressing cells after control (Figures 7A–7D) or hSlit2 treatment (Figures 7I–7L). In contrast, 5 min of human Slit2 treatment leads to a dramatic redistribution of Sos to the plasma membrane (Figures 7M, 7P, and 7G) and induces membrane ruffling (arrows in Figure 7O). In addition, on the membrane, Sos proteins are partially colocalized with hRobo1 receptors and F-actin (Figure 7P).

Similar results are observed in a *Drosophila* cell culture system. In Robo-expressing *Drosophila* S2R+ cells, an embryonic *Drosophila* cell line, endogenous Sos is localized in the cytoplasm (Figures S3A and S3B). In control-treated cells, very little colocalization between Robo and Sos is observed (Figures S3C and S3H). In contrast, Slit treatment leads to a considerable redistribution of Sos to the plasma membrane (Figures S3D and S3F). In these Slit-treated cells, we observe a striking increase in Robo and Sos colocalization in plasma membrane swellings that bear morphological similarity to membrane ruffles (Figures S3F and S3H). In addition, in Slit-treated cells Sos and Robo colocalization is observed in a large internal vesicular structure that may correspond to endocytosed receptor: the significance of this site of Sos and Robo colocalization is not clear (Figures S3D–S3F). Together with our biochemical data, these observations support the model that Slit triggers the formation of a protein complex on the plasma membrane consisting of Robo, Dock, and Sos. Once at the membrane, Sos would be poised to locally activate Rac to regulate the actin cytoskeleton, and in turn growth cone behavior.

Discussion

In this paper we present genetic and biochemical evidence that Sos is an important component of the Robo receptor signaling pathway. Specifically, our data support the idea that Sos provides a direct molecular link between the Robo receptor and the activation of Rac during *Drosophila* midline guidance. Genetic interactions between *sos*, *robo*, *dock*, *crGAP/vilse*, and the Rho family of small GTPases strongly suggest that Sos functions in vivo to regulate Rac activity during Robo signaling. Genetic rescue experiments indicate that *sos* is required specifically in neurons to mediate its axon guidance function. Furthermore, our genetic data establish that, in the context of midline axon guidance, the Ras-GEF and Rac-GEF activities of Sos can be functionally uncoupled. Biochemical experiments in cultured cells and *Drosophila* embryos show that Sos is recruited into a multiprotein complex consisting of the Robo receptor, the SH3-SH2 adaptor protein Dock, and Sos, in which Dock bridges the physical association between Robo and Sos. Finally, experiments in cultured cells support the idea that Slit activation of Robo can recruit Sos to the submembrane actin cytoskeleton to regulate cell morphology. Together, these results suggest a model in which Slit stimulation recruits Sos to the Robo receptor via Dock to regulate Rac-dependent cytoskeletal changes within the growth cone during axon repulsion.

Rho GTPase Substrate Specificity of Sos in Robo Signaling

Based on previous work implicating *rac* in Robo repulsion, as well as in vitro studies demonstrating that Sos exhibits GEF activity for Rac, but not Rho or Cdc42, Rac seemed the most likely Sos substrate. However, *rho* has also been implicated in mediating Robo repulsion (Fan et al., 2003; Fritz and VanBerkum, 2002), and genetic interactions between *sos* and dominant-negative *Rho* have been interpreted to suggest that Sos could act as a GEF for Rho. We have investigated this question further and have presented two types of genetic evidence that suggest that indeed Rac is the favored substrate of Sos. First, ectopic expression experiments in the eye reveal interactions exclusively between *sos* and *rac*. Second, genetic interaction experiments using loss of function mutations in *rac* and *rho* (rather than the more problematic dominant-negative forms of the GTPases) reveal strong dose-dependent interactions between *sos* and *rac*, but not *sos* and *rho* during midline axon guidance. Together, our observations argue in favor of Rac as the primary in vivo Sos substrate. Nevertheless, we cannot exclude the possibility that Sos also contributes to Rho activation and that the combined activation of Rac and Rho is instrumental in mediating the Robo response.

Sos as the Direct Molecular Link between Robo and Rac Activation

Previous studies from our lab and others' have demonstrated that Slit stimulation of the Robo receptor leads to a rapid increase in Rac activity in cultured cells. However, the mechanism by which Rac is activated downstream of Robo was not clear. Here we provide direct genetic and biochemical evidence that Sos is coupled to the Robo receptor through the Dock/Nck SH3-SH2 adaptor, where it can regulate local Rac activation. Studies in cultured mammalian cells have highlighted the importance of distinct Sos/adaptor protein complexes in controlling the subcellular localization and

(−; no interaction) during 24 hr in the presence of 80 g/ml X-Gal. Numbers indicate positions of the amino acids in the full-length protein. (C and F) Dock physically couples Sos to the Robo Receptor in 293Tcells. 293T cell lysates coexpressing His-Sos-Myc, HA-Dock, and HA-Robo (F) or HA-Dock and HA-Robo (C) were precipitated by Ni-NTA beads. The right two lanes show the coprecipitated proteins, while the left two lanes indicate Sos, Robo, and/or Dock expression in cells. In the presence of Dock, the interaction between Sos and Robo was detected (F), while in the absence of Dock, the interaction between Sos and Robo cannot be detected (C). (G) The presence of a Sos-Dock-Robo triple protein complex in *Drosophila* embryos. The right two lanes show the coprecipitated proteins, while the left two lanes indicate Robo, Dock, and Sos expression in embryos.

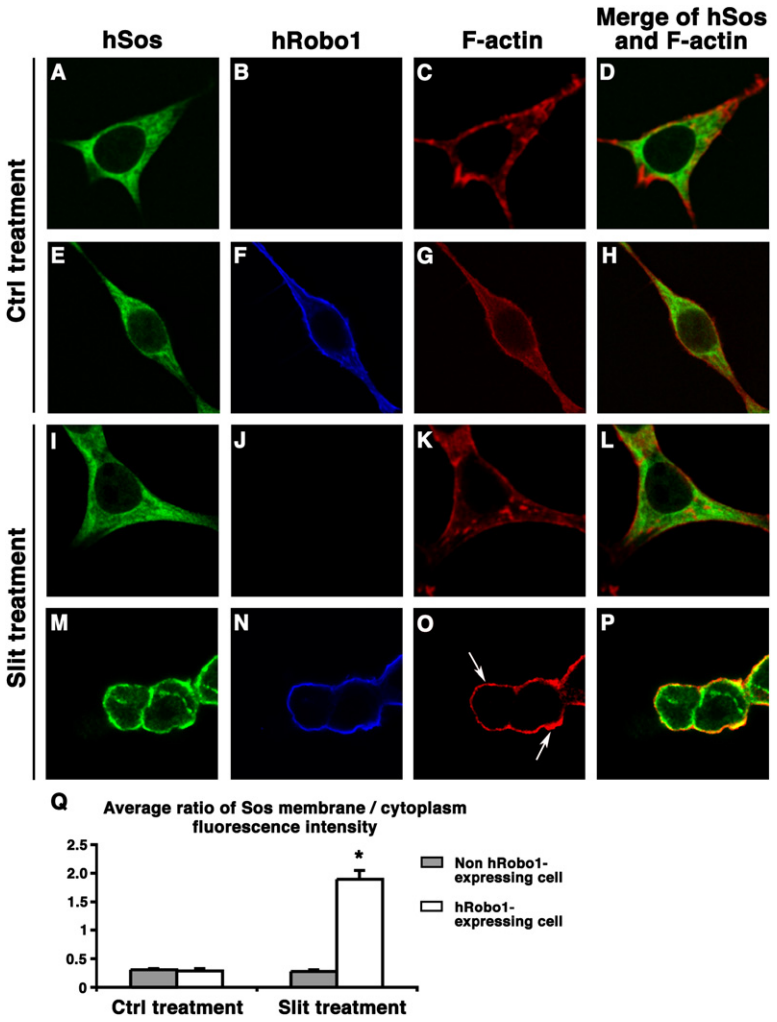

Figure 7. Human Slit2 Stimulation Recruits Human Sos to Membrane Robo Receptors and Induces Membrane Ruffling in 293T Cells

HEK293T cells transiently transfected with human MycHisRobo1. Endogenous hSos is visualized by rabbit anti-mSos1 antibodies (green), hRobo1 is visualized by mouse anti-myc antibodies (blue), and F-actin is visualized by Alexa 633-conjugated Phalloidin (red). A single confocal section is shown. (A–D) A non-hRobo1-expressing cell treated with control medium. The cell has long processes, as shown by F-actin staining, and hSos is predominantly localized in the cytoplasm. The membrane morphology and the cytoplasmic localization of hSos are not affected in either hRobo1-expressing cells treated with control medium (E–H) or in nontransfected cells treated with hSlit2-conditioned medium (I–L). (M–P) Two hRobo1-expressing cells treated with hSlit2-conditioned medium for 5 min. The membrane processes are retracted, linear membrane ruffles are induced (arrows in [O]), and hSos proteins are recruited to the membrane partially colocalizing with hRobo1 and F-actin (yellow in [P]). (Q) Quantification of the ratio of Sos membrane/cytoplasm fluorescence intensity in cells after control or Slit treatment. The average value of ten random cells from each group is shown on the y axis. The ratio of Sos membrane/cytoplasm fluorescence intensity in hRobo1-expressing cells was enhanced from 0.29 to 1.90 after hSlit2 treatment, while the ratio in nontransfected cells remained unchanged. The asterisk denotes that Sos redistribution to membrane in hRobo1-expressing cells by hSlit2 is of statistical significance ($p < 10^{-7}$, in a two-sample Student's t test). Error bars represent standard error of the mean.

substrate specificity of Sos. In the context of Rac activation, the E3b1 (Abi-1) adaptor has been shown to play a critical and rate-limiting role in Sos-dependent Rac activation and subsequent formation of membrane ruffles (Innocenti et al., 2002). Could Sos regulation of Rac activity during Robo repulsion be similarly limited by the availability of specific adaptor proteins? It is interesting to note in this context that overexpression of *dock* does not lead to ectopic axon repulsion, suggesting that Dock may not be limiting for Robo signaling. However, although *dock* mutants do have phenotypes indicative of reduced Robo repulsion, their phenotype is considerably milder than that seen in *robo* mutants, raising the possibility that there may be additional links between Robo and Sos.

A Ras-GEF-Independent Function of Sos in Axon Guidance

A number of studies in cultured mammalian cells have suggested that Rac activation induced by activated growth factor receptors requires the prior activation of Ras. For example, PDGF-induced membrane ruffling can be promoted or inhibited by expression of constitutively active or dominant-negative Ras, respectively (Nimnual et al., 1998; Scita et al., 1999). However, other studies have suggested that in Swiss 3T3 cell lines RTK activation of Rac is Ras independent (Ridley et al., 1992). In addition, the observation that Ras activation and Rac activation display very different kinetics, with Rac activation persisting long after Ras activity has returned to basal levels, has been used to argue against an obligate role for Ras in Rac activation (Innocenti et al., 2002). Here, using a genetic rescue approach, we have directly tested whether the ability of Sos to activate Rac during axon guidance in an intact organism requires its Ras-GEF function. Our genetic data indicate that the RasGEF domain of Sos is dispensable for axon guidance, while the DH RhoGEF domain is strictly required (Figure 5). This observation argues strongly in favor of the model that in vivo Sos activation of Rac does not strictly require Sos activation of Ras.

How Is the Rac-GEF Activity of Sos Regulated?

It is clear that subcellular localization plays a major role in regulating Sos activity and that different protein complexes containing Sos exist in different locations in the cell. Here we have shown that activation of the Robo receptor by Slit triggers the recruitment of Sos to Robo receptors at the plasma membrane. Our biochemical data argue that the adaptor Dock/Nck is instrumental in

bridging this interaction, and given the diverse interactions between Dock/Nck and guidance receptors, it seems likely that Dock/Nck could fulfill this role in many guidance receptor contexts. This bridging function of Dock/Nck and guidance receptors is analogous to the role of Grb2 for growth factor receptors only insomuch as it brings signaling molecules to the receptor—the mechanism of interaction is distinct, since it is mediated through SH3 domain contacts rather than SH2/phosphotyrosine interactions. Our observations suggest that there may be an additional pool of Sos that can function in a distinct adaptor protein/guidance receptor complex to regulate cell morphology in response to extracellular guidance cues.

Could Abl Regulate the Rac-Specific GEF Activity of Sos?

Is regulating subcellular localization the only mechanism by which Sos activity is controlled? This seems unlikely. Indeed, a recent study has implicated tyrosine phosphorylation of Sos by Abl as an additional mechanism to activate the Rac-specific GEF activity of Sos in vertebrate cell culture models (Sini et al., 2004). This raises the intriguing possibility that Abl may fulfill a similar role for Robo signaling. This is a particularly appealing idea given the well-documented genetic and physical interactions between Robo and Abl (Bashaw et al., 2000; Hsouna et al., 2003; Wills et al., 2002). Indeed, we have observed that *sos* and *abl* exhibit dose-dependent genetic interactions during midline axon guidance (L.Y. and G.J.B., unpublished data). A clear genetic test of whether Abl activates the Rac-GEF activity of Sos downstream of Robo may be complicated by the fact that Abl appears to play a dual role in Robo repulsion: both increasing and decreasing *abl* function lead to disruptions in Robo function. Nevertheless, it should be possible in the future to generate mutant versions of Sos that are refractory to Abl activation and to test whether these alterations disrupt the Sos guidance function. It will also be of great interest to determine whether the redistribution of Sos can also be observed in response to guidance receptor signaling in navigating growth cones, and if so, then what changes in actin dynamics and growth cone behavior are elicited.

Experimental Procedures

Molecular Biology

Drosophila Sos was PCR amplified from EST clone #GH01796 (DGRC) and subcloned into the pUAST vector. A 6-myc tag was PCR amplified and subcloned to the C terminus of Sos to generate a pUAST-Sosmyc construct. SosΔDHmyc lacking the DH domain (aa 251–432) and SosΔRasGEFmyc lacking the RasGEF domain (aa 824–1066) were generated by PCR mutagenesis and subcloned into the pUAST vector. Sosmyc was also subcloned into the pCDNA3.1-His vector (Invitrogen) to generate pCDNA3.1-His-Sosmyc. Different fragments of Sos (aa 1–600; aa 601–1079; aa 1080–1595) were cloned into the pJG4-5 vector. All constructs were sequenced.

Genetics

The following fly strains were used: *sos^{e2H}/CyOWgβGal*, *sos^{e4G}/CyOWgβGal*, *slit^{2}/CyOWgβGal*, *robo^{GA285}/CyOWgβGal*, *rac1^{J11}/TM6UbxβGal*, *rhoA^{220}/CyOWgβGal*, *dock^{3}/CyOWgβGal*, *ena^{GC1}/CyOWgβGal*, and *UASCrGAP, elavGal4/TM3UbxβGal*. For the genetic interaction and rescue experiments, the following stocks were generated: (1) *sos^{e2H}, slit^{2}/CyOWgβGal*, (2) *sos^{e2H}, robo^{GA285}/CyOWgβGal*, (3) *sos^{e2H}, rhoA^{220}/CyOWgβGal*, (4) *sos^{e2H}/CyOElavβGal; rac1^{J11}/TM6UbxβGal*, (5) *sos^{e2H}/CyOWgβGal; UASRac^{N17}*, (6) *sos^{e2H}/CyOWgβGal; UASRho^{N19}*, (7) *sos^{e4G}/CyOWgβGal; elavGal4*, (8) *sos^{e4G}/CyOWgβGal; ftz^{ng}Gal4/TM2*, (9) *sos^{e2H}, rhoA^{220}/CyOWgβGal; elavGal4*, (10) *sos^{e2H}/CyOElavβGal; UASCrGAP, elavGal4/TM3UbxβGal*, (11) *UASSosmyc; UASCrGAP, elavGal4/TM3UbxβGal*, (12) *sos^{e2H}, dock^{3}/CyOWgβGal*, (13) *sos^{e2H}, ena^{GC1}/CyOWgβGal*. *sos^{e2H}* and *sos^{e4G}* contain premature stop codons at amino acid positions 579 and 421, respectively, and have previously been demonstrated to be null mutations. To generate transgenic fly strains, *UASSos*, *UASSosmyc*, *UASSosΔDHmyc*, and *UASSos ΔRasGEFmyc* were transformed into *w^{1118}* flies using standard procedures. Independent transformant lines on the second and third chromosome were obtained. The Gal4-UAS system was used to express transgenes in the Ftz ipsilateral neurons (*ftz^{ng}Gal4*) or in all neurons (*elavGal4*). Crosses to *GMRGal4* to generate "rough eye" phenotypes were conducted at 18°C. All other crosses were conducted at 25°C.

Immunohistochemistry

HRP immunohistochemistry was performed as previously described, and images were obtained using a Zeiss Axiocam and Openlab software (Improvision). Fluorescent staining for FasII guidance defects was performed using mouse MAb 1D4 (1:100) and antibodies against β-gal (mouse anti-β-gal 1:150, rabbit anti-β-gal 1:10,000; Roche). β-gal staining allowed the identification of genotypes in embryos. Cy3 secondary antibody (Molecular Probes) was used at 1:1000, and Alexa Fluor 488 secondary antibody was used at 1:500–1000. Fluorescence double-staining for Sos and BP102 was performed using rabbit anti-Sos (1:500; a gift from Dr. U. Banerjee) and mouse MAb BP102 (1:100). Fluorescent images were taken using a Leica Confocal TCS SL microscope and processed by NIH Image J software.

Immunoprecipitation

293T cells were transfected with plasmid DNA at 90% confluency using Effectene Transfection Reagent (Qiagen). Twenty-four hours posttransfection, cells were lysed in lysis buffer containing 1% Triton X-100, 150 mM NaCl, 50 mM Tris (pH 8.0), 10 mM Imidazole, 2× protease inhibitor (Roche), and 1 mM $NaVO_3$. Cell lysates were incubated with Ni-NTA resin (Qiagen) at 4°C for 2 hr to precipitate His-Sosmyc. The resin was washed three times with lysis buffer and heated at 100°C for 10 min. The precipitates were resolved on SDS-PAGE gels and blotted with mouse anti-HA antibody (1:1000; Covance) and mouse anti-myc antibody (9E10; 1:1000). For in vivo IP, lysates were prepared from 100 μl of embryos overexpressing one copy of *UASRobomyc* in all neurons. Embryos were smashed in lysis buffer containing 0.5% Triton X-100, 1× PBS, 2× protease inhibitor, and 1 mM $NaVO_3$ and were incubated with mouse anti-myc antibody and protein A Sepharose 4B beads at 4°C for 3 hr. Beads were washed three times with lysis buffer, heated at 100°C for 10 min, resolved on SDS-PAGE gels, and blotted with rabbit anti-Sos antibody (1:2000), rabbit anti-Dock antibody (1:4000), and mouse anti-myc antibody.

GST Pull-Down

GST and GST-Dock were expressed in *E. coli* and purified using the Bulk and RediPack purification modules (Amersham). His-Sosmyc was expressed in 293T cells, and cells were lysed in lysis buffer containing 1% Triton X-100, 150 mM NaCl, 50 mM Tris (pH 7.5), 2× protease inhibitor, and 1 mM $NaVO_3$. Cell lysates were incubated with Glutathione Sepharose 4B beads bound to 5 μg GST or GST Dock at 4°C for 2 hr. The beads were washed three times with lysis buffer and heated at 100°C for 10 min. Precipitated proteins were resolved on SDS-PAGE gels and blotted with mouse anti-myc antibody.

Cell Immunofluorescence

HEK293T Cells

293T cells were seeded on glass coverslips coated with poly-L-lysine and transfected with plasmid DNA at 40% confluency using Effectene Transfection Reagent (Qiagen). Twenty-four hours after transfection, cells were starved in serum-free DMEM for 12–16 hr and then stimulated with conditioned medium of hSlit2-stably-expressing 293T cells (a gift from Dr. Y Rao) for 5 min. Treated cells

were washed with 1× PBS once and immediately fixed in 4% paraformaldehyde/1× PBS for 20 min. Fixed cells were permeabilized in 0.1% Triton X-100/1× PBS for 2 min and blocked with 3% BSA/1× PBS for 5 min. Cells were then incubated with primary antibody (rabbit anti-hSos 1:50, mouse anti-myc 1:1000) overnight at 4°C, and secondary antibody (rabbit Alexa Fluor 488, mouse Cy3 secondary antibody) for 30 min at RT, respectively. Finally, cells were stained with Alexa 633-conjugated phalloidin for 1 hr at RT. Fluorescent images were taken using a Leica Confocal TCS SL microscope and processed by NIH Image J software.

Quantification of Sos Membrane/Cytoplasm Fluorescence Intensity

For each group of cells, ten random cells were selected for quantification. Fluorescence intensity is calculated by area (pixel numbers) multiplied by average fluorescence intensity using NIH Image J software. In 293T cells, actin staining was processed to generate a membrane mask for all cells. The overlapping area of membrane mask and Sos staining is used to calculate Sos membrane fluorescence intensity. The cytoplasmic area is calculated by nonoverlapping Sos staining area minus nucleus area.

Supplemental Data

The Supplemental Data include Supplemental Experimental Procedures, three supplemental figures, and one supplemental table and can be found with this article online at http://www.neuron.org/cgi/content/full/52/4/595/DC1/.

Acknowledgments

The authors would like to thank Liqun Luo, Mike Simon, Utpal Banerjee, Yi Rao, Ilaria Rebay, Barry Dickson, and Giorgio Scita for various fly stocks and reagents. We thank Nan Liu for help obtaining images of *Drosophila* eyes. We thank members of the Bashaw lab, especially Juan Pablo Labrador, David Garbe, and Ming Li, for many helpful discussions. This work was supported by National Institutes of Health grant NS046333 to G.J.B.

Received: May 19, 2006
Revised: September 13, 2006
Accepted: September 29, 2006
Published: November 21, 2006

References

Bashaw, G.J., Kidd, T., Murray, D., Pawson, T., and Goodman, C.S. (2000). Repulsive axon guidance: Abelson and Enabled play opposing roles downstream of the roundabout receptor. Cell *101*, 703–715.

Bonfini, L., Karlovich, C.A., Dasgupta, C., and Banerjee, U. (1992). The Son of sevenless gene product: A putative activator of Ras. Science *255*, 603–606.

Brand, A.H., and Perrimon, N. (1993). Targeted gene expression as a means of altering cell fates and generating dominant phenotypes. Development *118*, 401–415.

Cowan, C.W., Shao, Y.R., Sahin, M., Shamah, S.M., Lin, M.Z., Greer, P.L., Gao, S., Griffith, E.C., Brugge, J.S., and Greenberg, M.E. (2005). Vav family GEFs link activated Ephs to endocytosis and axon guidance. Neuron *46*, 205–217.

Dickson, B.J. (2001). Rho GTPases in growth cone guidance. Curr. Opin. Neurobiol. *11*, 103–110.

Englund, C., Steneberg, P., Falileeva, L., Xylourgidis, N., and Samakovlis, C. (2002). Attractive and repulsive functions of Slit are mediated by different receptors in the Drosophila trachea. Development *129*, 4941–4951.

Fan, X., Labrador, J.P., Hing, H., and Bashaw, G.J. (2003). Slit stimulation recruits Dock and Pak to the roundabout receptor and increases Rac activity to regulate axon repulsion at the CNS midline. Neuron *40*, 113–127.

Fritz, J.L., and VanBerkum, M.F. (2000). Calmodulin and son of sevenless dependent signaling pathways regulate midline crossing of axons in the Drosophila CNS. Development *127*, 1991–2000.

Fritz, J.L., and VanBerkum, M.F. (2002). Regulation of rho family GTPases is required to prevent axons from crossing the midline. Dev. Biol. *252*, 46–58.

Hakeda-Suzuki, S., Ng, J., Tzu, J., Dietzl, G., Sun, Y., Harms, M., Nardine, T., Luo, L., and Dickson, B.J. (2002). Rac function and regulation during Drosophila development. Nature *416*, 438–442.

Hariharan, I.K., Hu, K.Q., Asha, H., Quintanilla, A., Ezzell, R.M., and Settleman, J. (1995). Characterization of rho GTPase family homologues in Drosophila melanogaster: Overexpressing Rho1 in retinal cells causes a late developmental defect. EMBO J. *14*, 292–302.

Hing, H., Xiao, J., Harden, N., Lim, L., and Zipursky, S.L. (1999). Pak functions downstream of Dock to regulate photoreceptor axon guidance in *Drosophila*. Cell *97*, 853–863.

Hsouna, A., Kim, Y.S., and VanBerkum, M.F. (2003). Abelson tyrosine kinase is required to transduce midline repulsive cues. J. Neurobiol. *57*, 15–30.

Hu, Q., Milfay, D., and Williams, L.T. (1995). Binding of NCK to SOS and activation of ras-dependent gene expression. Mol. Cell. Biol. *15*, 1169–1174.

Hu, H., Li, M., Labrador, J.P., McEwen, J., Lai, E.C., Goodman, C.S., and Bashaw, G.J. (2005). Cross GTPase-activating protein (CrossGAP)/Vilse links the Roundabout receptor to Rac to regulate midline repulsion. Proc. Natl. Acad. Sci. USA *102*, 4613–4618.

Innocenti, M., Tenca, P., Frittoli, E., Faretta, M., Tocchetti, A., Di Fiore, P.P., and Scita, G. (2002). Mechanisms through which Sos-1 coordinates the activation of Ras and Rac. J. Cell Biol. *156*, 125–136.

Innocenti, M., Frittoli, E., Ponzanelli, I., Falck, J.R., Brachmann, S.M., Di Fiore, P.P., and Scita, G. (2003). Phosphoinositide 3-kinase activates Rac by entering in a complex with Eps8, Abi1, and Sos-1. J. Cell Biol. *160*, 17–23.

Kidd, T., Brose, K., Mitchell, K.J., Fetter, R.D., Tessier-Lavigne, M., Goodman, C.S., and Tear, G. (1998). Roundabout controls axon crossing of the CNS midline and defines a novel subfamily of evolutionarily conserved guidance receptors. Cell *92*, 205–215.

Kidd, T., Bland, K.S., and Goodman, C.S. (1999). Slit is the midline repellent for the robo receptor in *Drosophila*. Cell *96*, 785–794.

Kramer, S.G., Kidd, T., Simpson, J.H., and Goodman, C.S. (2001). Switching repulsion to attraction: Changing responses to slit during transition in mesoderm migration. Science *292*, 737–740.

Long, H., Sabatier, C., Ma, L., Plump, A., Yuan, W., Ornitz, D.M., Tamada, A., Murakami, F., Goodman, C.S., and Tessier-Lavigne, M. (2004). Conserved roles for Slit and Robo proteins in midline commissural axon guidance. Neuron *42*, 213–223.

Lundstrom, A., Gallio, M., Englund, C., Steneberg, P., Hemphala, J., Aspenstrom, P., Keleman, K., Falileeva, L., Dickson, B.J., and Samakovlis, C. (2004). Vilse, a conserved Rac/Cdc42 GAP mediating Robo repulsion in tracheal cells and axons. Genes Dev. *18*, 2161–2171.

Luo, L. (2000). Rho GTPases in neuronal morphogenesis. Nat. Rev. Neurosci. *1*, 173–180.

Luschnig, S., Moussian, B., Krauss, J., Desjeux, I., Perkovic, J., and Nusslein-Volhard, C. (2004). An F1 genetic screen for maternal-effect mutations affecting embryonic pattern formation in Drosophila melanogaster. Genetics *167*, 325–342.

Matsuura, R., Tanaka, H., and Go, M.J. (2004). Distinct functions of Rac1 and Cdc42 during axon guidance and growth cone morphogenesis in Drosophila. Eur. J. Neurosci. *19*, 21–31.

Ng, J., Nardine, T., Harms, M., Tzu, J., Goldstein, A., Sun, Y., Dietzl, G., Dickson, B.J., and Luo, L. (2002). Rac GTPases control axon growth, guidance and branching. Nature *416*, 442–447.

Nimnual, A., and Bar-Sagi, D. (2002). The two hats of SOS. Sci. STKE *2002*, PE36.

Nimnual, A.S., Yatsula, B.A., and Bar-Sagi, D. (1998). Coupling of Ras and Rac guanosine triphosphatases through the Ras exchanger Sos. Science *279*, 560–563.

Nolan, K.M., Barrett, K., Lu, Y., Hu, K.Q., Vincent, S., and Settleman, J. (1998). Myoblast city, the Drosophila homolog of DOCK180/CED-5, is required in a Rac signaling pathway utilized for multiple developmental processes. Genes Dev. *12*, 3337–3342.

Oinuma, I., Ishikawa, Y., Katoh, H., and Negishi, M. (2004a). The Semaphorin 4D receptor Plexin-B1 is a GTPase activating protein for R-Ras. Science *305*, 862–865.

Oinuma, I., Katoh, H., and Negishi, M. (2004b). Molecular dissection of the semaphorin 4D receptor plexin-B1-stimulated R-Ras GTPase-activating protein activity and neurite remodeling in hippocampal neurons. J. Neurosci. *24*, 11473–11480.

Okada, S., and Pessin, J.E. (1996). Interactions between Src homology (SH) 2/SH3 adapter proteins and the guanylnucleotide exchange factor SOS are differentially regulated by insulin and epidermal growth factor. J. Biol. Chem. *271*, 25533–25538.

Patel, B.N., and Van Vactor, D.L. (2002). Axon guidance: The cytoplasmic tail. Curr. Opin. Cell Biol. *14*, 221–229.

Ridley, A.J., Paterson, H.F., Johnston, C.L., Diekmann, D., and Hall, A. (1992). The small GTP-binding protein rac regulates growth factor-induced membrane ruffling. Cell *70*, 401–410.

Scita, G., Nordstrom, J., Carbone, R., Tenca, P., Giardina, G., Gutkind, S., Bjarnegard, M., Betsholtz, C., and Di Fiore, P.P. (1999). EPS8 and E3B1 transduce signals from Ras to Rac. Nature *401*, 290–293.

Scita, G., Tenca, P., Frittoli, E., Tocchetti, A., Innocenti, M., Giardina, G., and Di Fiore, P.P. (2000). Signaling from Ras to Rac and beyond: Not just a matter of GEFs. EMBO J. *19*, 2393–2398.

Scita, G., Tenca, P., Areces, L.B., Tocchetti, A., Frittoli, E., Giardina, G., Ponzanelli, I., Sini, P., Innocenti, M., and Di Fiore, P.P. (2001). An effector region in Eps8 is responsible for the activation of the Rac-specific GEF activity of Sos-1 and for the proper localization of the Rac-based actin-polymerizing machine. J. Cell Biol. *154*, 1031–1044.

Seeger, M., Tear, G., Ferres-Marco, D., and Goodman, C.S. (1993). Mutations affecting growth cone guidance in *Drosophila*: Genes necessary for guidance toward or away from the midline. Neuron *10*, 409–426.

Shamah, S.M., Lin, M.Z., Goldberg, J.L., Estrach, S., Sahin, M., Hu, L., Bazalakova, M., Neve, R.L., Corfas, G., Debant, A., and Greenberg, M.E. (2001). EphA receptors regulate growth cone dynamics through the novel guanine nucleotide exchange factor ephexin. Cell *105*, 233–244.

Silver, S.J., Chen, F., Doyon, L., Zink, A.W., and Rebay, I. (2004). New class of Son-of-sevenless (Sos) alleles highlights the complexities of Sos function. Genesis *39*, 263–272.

Simon, M.A., Bowtell, D.D., Dodson, G.S., Laverty, T.R., and Rubin, G.M. (1991). Ras1 and a putative guanine nucleotide exchange factor perform crucial steps in signaling by the sevenless protein tyrosine kinase. Cell *67*, 701–716.

Sini, P., Cannas, A., Koleske, A.J., Di Fiore, P.P., and Scita, G. (2004). Abl-dependent tyrosine phosphorylation of Sos-1 mediates growth-factor-induced Rac activation. Nat. Cell Biol. *6*, 268–274.

Wills, Z., Emerson, M., Rusch, J., Bikoff, J., Baum, B., Perrimon, N., and Van Vactor, D. (2002). A *Drosophila* homolog of cyclase-associated proteins collaborates with the Abl tyrosine kinase to control midline axon pathfinding. Neuron *36*, 611–622.

Wong, K., Ren, X.R., Huang, Y.Z., Xie, Y., Liu, G., Saito, H., Tang, H., Wen, L., Brady-Kalnay, S.M., Mei, L., et al. (2001). Signal transduction in neuronal migration: Roles of GTPase activating proteins and the small GTPase Cdc42 in the Slit-Robo pathway. Cell *107*, 209–221.

Yu, T.W., and Bargmann, C.I. (2001). Dynamic regulation of axon guidance. Nat. Neurosci. *4* (*Suppl*), 1169–1176.

Yu, T.W., Hao, J.C., Lim, W., Tessier-Lavigne, M., and Bargmann, C.I. (2002). Shared receptors in axon guidance: SAX-3/Robo signals via UNC-34/Enabled and a Netrin-independent UNC-40/DCC function. Nat. Neurosci. *5*, 1147–1154.

Yuan, X.B., Jin, M., Xu, X., Song, Y.Q., Wu, C.P., Poo, M.M., and Duan, S. (2003). Signalling and crosstalk of Rho GTPases in mediating axon guidance. Nat. Cell Biol. *5*, 38–45.